Strong Bragg Gratings in Highly Photosensitive Photo-Thermo-Refractive-Glass Optical Fiber

Peter Hofmann, Rodrigo Amezcua-Correa, Enrique Antonio-Lopez, Daniel Ott, Marc SeGall, Ivan Divliansky, Julien Lumeau, Larissa Glebova, Leonid Glebov, N. Peyghambarian, and Axel Schülzgen

***Abstract*— A new type of photosensitive fiber is demonstrated. Long lengths (> 100 m) of coreless optical fiber are fabricated from highly photosensitive photo-thermo-refractive glass. A minimum loss of < 2 dB/m is measured. A holographic technique using low power near-UV two-beam interference patterns is applied to record strong and robust Bragg gratings inside the fiber. The gratings show no degradation when heated up to 425 °C for several hours.**

***Index Terms*— Fiber Bragg grating, optical fiber fabrication, photo thermo refractive glass, photosensitivity.**

I. Introduction

FIBER Bragg gratings (FBGs) are optical components of significant interest due to their multitude of applications in communications, fiber optic sensing, and fiber lasers [1], [2]. Therefore, FBGs have been the subject of an enormous body of research particularly following the first demonstration of transverse holographic grating writing in 1989 [3]. This has led to a number of different types of FBGs, which are often classified with respect to their underlying formation mechanism [4]. Type-1 gratings, which are formed by exposure of germanium doped silica fibers to fringed UV radiation are an established technology and dominate the grating landscape to date. Nevertheless, research into novel fibers for FBG fabrication continues, to enhance photosensitivity and increase the obtainable refractive index (RI) modulation as well as to improve the stability of FBGs with respect to elevated temperatures, harsh environments, and high optical power densities. To achieve these goals, many studies focus on novel doping materials. For instance, BGe co-doped fibers have been reported to provide higher levels of photosensitivity [5], and hydrogen loading can further enhance this property [6]. However, gratings written in these fibers are reported to have even poorer temperature stability and additional losses at wavelengths around 1550 nm can be introduced [7]–[10]. As another example, studies of Sn-doped fiber have shown some promise regarding improved thermal stability of FBGs in particular when post fabrication treatments are applied [11]–[14]. Type-IIa gratings have been shown to withstand temperatures of 700 °C [15]. Higher temperature resistance can be achieved with Type-II gratings written with UV excimer lasers [16] or more recently with IR-femtosecond lasers [17], [18]. Although they still have low reflectivities, chemical composition gratings (CCG) [19] and regenerated gratings [20] have shown to withstand extreme temperatures of 1000 °C.

In this letter, we demonstrate a novel alternative approach to the fabrication of strong and stable FBGs utilizing optical fiber made of highly photosensitive photo-thermo-refractive (PTR) glass. PTR glass is a sodium-zinc-aluminum-silicate glass doped with anions (fluorine and bromine) and cations (antimony, tin, cerium, and silver) [21]. This glass changes its RI after exposure to near UV radiation (300–350 nm) followed by a thermal treatment in the vicinity of 500 °C. It shows high photosensitivity (induced RI change of 10^{-3} for exposure at 325 nm below 1 J/cm2), high thermal stability of a recorded phase pattern (up to 400 °C), and high tolerance to optical and ionizing irradiation. Basic optical and thermo-mechanical properties of PTR glass are described in Refs. [22], [23].

PTR bulk glass is successfully used for volume hologram recording with a wide range of applications including spectral narrowing of laser diodes, spectral beam combining, and temporal compression of laser pulses [22], [24], [25]. Optical fiber fabricated from PTR glass combines the promises of high index changes, elevated operation temperatures, very high optical damage thresholds, and the ability to create complex holographic structures beyond conventional FBGs [21]. Holograms in PTR glass can be recorded with commercially available portable He-Cd lasers. This simplifies the FBG fabrication process, since bulky UV excimer lasers and phase masks become unnecessary.

Our PTR fiber fabrication efforts were additionally motivated by a previous experiment which demonstrated that fiber strands directly obtained from a PTR glass melt can retain photosensitivity comparable to that of the bulk glass [26]. Here we report for the first time the fabrication of tens of meters of coreless optical fiber made from PTR glass by a well-controlled fiber drawing process utilizing a PTR glass preform and a conventional fiber draw tower. The PTR fiber's relatively low propagation loss and excellent mechanical

Manuscript received August 22, 2012; revised October 6, 2012; accepted October 29, 2012. Date of publication November 15, 2012; date of current version December 18, 2012. This work was supported in part by the Air Force Office of Scientific Research under Grant W911NF-10-1-0441 and in part by the Center for Integrated Access Networks at the University of Arizona.

P. Hofmann and N. Peyghambarian are with the College of Optical Sciences, University of Arizona, Tucson, AZ 30332 USA (e-mail: phofmann@optics.arizona.edu; nnp@optics.arizona.edu).

R. Amezcua-Correa, E. Antonio-Lopez, D. Ott, M. SeGall, I. Divliansky, J. Lumeau, L. Glebova, L. Glebov, and A. Schülzgen are with CREOL, the College of Optics and Photonics, University of Central Florida, Orlando, FL 32816 USA (e-mail: r.amezcua@creol.ucf.edu; jealopez@creol.ucf.edu; dott@creol.ucf.edu; msegall@creol.ucf.edu; ibd1@creol.ucf.edu; jlumeau@creol.ucf.edu; lglebova@creol.ucf.edu; axel@creol.ucf.edu).

Color versions of one or more of the figures in this letter are available online at http://ieeexplore.ieee.org.

Digital Object Identifier 10.1109/LPT.2012.2227308

strength enable the fabrication of various fiber optic components. By writing high reflectivity FBGs into the PTR glass fiber we demonstrate that the photosensitivity is maintained during the fiber fabrication process. The fabricated FBGs do not degrade when heated to temperatures up to 425 °C for several hours. Our study opens new avenues for the development of PTR glass fiber optic structures with well-defined RI distributions that provide the stability and robustness required by many applications.

II. Experiments

The PTR glass was prepared by melting high purity chemicals in a platinum crucible at 1460 °C. The glass composition used for the fiber was $15Na_2O - 5ZnO - 3Al_2O_3 - 70SiO_2 - 6NaF - 1KBr - 0.02Ag_2O - 0.01CeO_2 - 0.01SnO_2 - 0.03Sb_2O_3$ (mol%). To ensure homogenization the melt was continuously stirred for 3 hours. The glass was then annealed for several hours at 460 °C and cooled down to room temperature over a period of 20 hours. The RI homogeneity throughout the glass slab used for preform fabrication was better than 40 ppm (4×10^{-5}). The photosensitivity of this glass (maximum achievable RI changes after UV exposure and thermal development) is up to 700 ppm (7×10^{-4}), indicating the glass is well suited for hologram recording. The raw glass slab was then turned into a cylindrical rod of 8 mm diameter and 75 mm length using a lathe and a counter rotating diamond tool. The lathe was operating at 190 rpm. The tool was spinning at 4000 rpm and the lathe feedrate was set to 20 mm/min. Finally, the rod was polished in four steps where the grain size was successively reduced to minimize surface roughness. Fig. 1(a) shows a photograph of the PTR glass slab and the finished preform. This preform was then drawn into a coreless multi-mode fiber (MMF), using a customized draw tower (Heathway). The diameter has been successively changed from 135 μm to 60 μm during the drawing process. A micrograph of the cross-section of a sample with 115 μm diameter is shown in the inset of Fig. 1(a). Even without coating, this PTR glass fiber exhibits good mechanical stability.

The RI profiles of the fibers have been measured using a fiber analyzer (Interfiber Analysis IFA-100). An example of a RI profile at a wavelength of 1032 nm of a PTR fiber measuring 105 μm in diameter is shown in the inset of Fig. 1(b). Since the fiber has no core, the profile is essentially flat. Also shown in Fig. 1(b) is the wavelength dependence of the RI for 3 fibers with different diameters, which was also obtained from the above mentioned fiber analyzer.

The spectral attenuation of the PTR glass fibers has been determined using the conventional cutback method. The experimental setup is shown in Fig. 1(c). White light from a super-continuum source (NKT photonics SuperK compact) was launched through a standard MMF with 105/125 μm core/cladding diameter and a NA of 0.22. A PTR glass fiber sample of 1.1 m length was fusion spliced to the MMF on both ends, and the transmitted light was guided into a Yokogawa AQ6370B optical spectrum analyzer (OSA) operating at a resolution bandwidth of 2 nm. The splicing was done on a

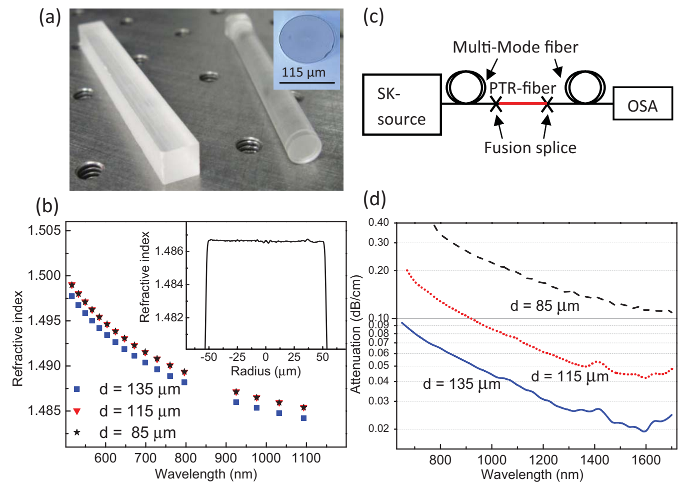

Fig. 1. PTR glass slab and finished preform. (a) Cross section of a coreless PTR fiber. Inset: micrograph of the cross section of a sample with 115 μm diameter. (b) Measured wavelength dependence of RI for PTR glass fibers with different diameters. Inset: example of a measured RI profile. (c) Experimental setup for spectral attenuation measurements. (d) Measured spectral attenuation of PTR glass fibers with different diameters.

commercial fusion splicer (Ericsson FSU 995) with a modified splice recipe to account for the different thermal properties of the two glasses. This resulted in mechanically robust splices with measured losses as low as 0.5 dB per splice for PTR fiber diameters similar to the 105 μm core diameter of the MMF. After each measurement the length of PTR glass fiber was reduced in steps of 10 cm. The fiber end was then re-spliced to the collecting fiber. As shown in Fig. 1(d) the fiber attenuation systematically decreases with the increasing fiber diameter indicating surface scattering as the dominant loss mechanism. The minimum attenuation is slightly less than 0.02 dB/cm at 1550 nm for a fiber diameter of 135 μm. Increased losses around 1400 nm are related to the two-phonon OH vibrational mode. At longer wavelengths the on-set of the single phonon vibrational absorption of OH admixture with maximum at 2.8 μm is visible.

In order to test if the photosensitivity of the glass was affected by the fiber drawing process, FBGs have been inscribed into several samples of the PTR glass fiber. The recording process for PTR-FBGs is the same as that used for recording volume Bragg gratings (VBG) into bulk PTR glass fiber [22]. At first, the samples were exposed for about 200 s to a two beam interference pattern from a CW He-Cd laser operating at 325 nm. Both beams had a round top-hat profile with a diameter of 28 mm, and with a half angle of interference of 8.3° the resulting FBG was approximately 30 mm long. The grating period was designed to obtain a Bragg wavelength around 1535 nm. After exposure, the samples underwent a thermal development for 1 hour at 515 °C [22]. The fibers were then cleaved close to the grating region and spliced to single-mode fiber (Corning smf28e). Subsequently transmission spectra where measured using again the super-continuum source and the OSA, now operating at a resolution bandwidth of 20 pm.

Backscattering was measured using a smf28e-coupled Lunatech OBR4400 optical backscatter reflectometer (OBR), operating with a spatial and spectral resolution of 0.1 mm

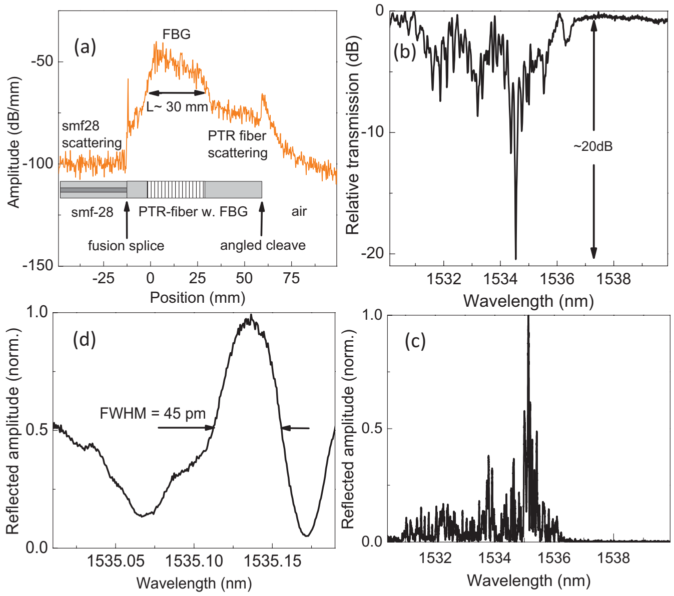

Fig. 2. Back-scattered amplitude as a function of position along the fiber. (a) Length of the FBG is approximately 30 mm, while the whole PTR glass fiber segment is about 70-mm long. (b) Transmission spectra of a PTR glass FBG with the grating filters out 20 dB in transmission. (c) Reflection spectrum of a PTR glass FBG. (d) High resolution reflection spectrum of the same PTR glass FBG around the Bragg wavelength. The FWHM of the main Bragg peaks spectral width is 45 pm.

and 5 pm respectively. The FBG was again fusion spliced to smf28e fiber. Fig. 2(a) shows the measurement trace from the OBR in the spatial domain. The PTR-fiber was angle cleaved at the glass-air interface to avoid Fabry-Perot effects. For illustration a schematic of the fiber chain is displayed below the OBR-trace. Clearly visible is the peak, marking the fusion splice between the smf28e and the 70 mm long section of PTR fiber. The section from 0−30 mm with the highest backscatter amplitude indicates the location of the FBG. The length of 30 mm is consistent with the size of the UV-interference pattern used for hologram recording. The FBG is followed by a section of unexposed PTR-fiber, indicated by the reduced background loss between the FBG and the angle-cleave. The measured transmission spectrum of a PTR glass FBG is shown in Fig. 2(b). The depth of the main transmission minimum is −20 dB. The width is limited by the OSA resolution. To determine the width of the main Bragg peak we use OBR measurements in the spectral domain shown in Fig. 2(c) and (d) where Fig. 2(d) is a zoom in of Fig. 2(c). The multiple peaks next to the main Bragg peaks are due to the multi-mode nature of the fiber; each excited mode has its characteristic Bragg wavelength. The subtle difference of the Bragg wavelengths in the transmission and reflection spectra can be explained by slightly different coupling conditions for the reflected and the transmitted wave at the splices between smf28e and PTR glass fiber.

The PTR glass FBGs have been tested for robustness at elevated temperatures. The temperature has been increased in steps of 50 K from room temperature to 450 °C. The transmission spectra at each temperature have been measured. The main Bragg wavelength depends linearly on temperature and shifts with a slope of 15.6 pm/K as shown in Fig. 3(a). For comparison, a similar experiment has been performed with

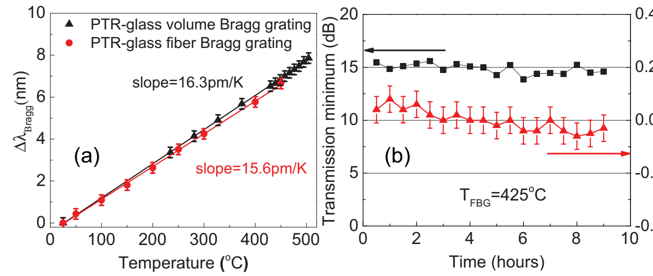

Fig. 3. (a) Bragg wavelength shift as a function of grating temperature for a PTR glass FBG (red) and for comparison for a PTR-bulk glass VBG. (b) Measurement of transmission minimum (black) and Bragg wavelength (red) of a PTR glass FBG that was exposed for 9 hours to 425 °C ambient temperature.

a VBG fabricated in bulk PTR glass. The result is also plotted in Fig. 3(a). The VBG exhibited a slope of 16.3 pm/K. The difference of only 0.7 pm/K between the two slopes is within the error margin of the FBGs and VBGs heating experiment, suggesting that the Bragg wavelength of PTR glass FBGs and PTR glass VBGs shifts at the same rate which is determined mainly by thermal expansion of PTR glass, which is about 9.5 ppm/K. To demonstrate long term stability, PTR glass FBGs where heated up to a temperature of 425 °C. After allowing the temperature to stabilize, we measured the FBG's transmission spectrum over a time window of 9 hours. In Fig. 3(b) the transmission minimum and the Bragg wavelength of each transmission spectrum are plotted. Both changed only slightly over the duration of the experiment, clearly showing high durability in a harsh environment.

III. Conclusion

In conclusion, we report the first fabrication of multi-mode low loss coreless fibers drawn from a solid PTR glass preform. We further demonstrate strong and robust high efficiency fiber Bragg gratings recorded by a holographic technique. The gratings show high stability at elevated temperatures up to 425 °C. Such fibers open exciting new avenues for the development of holographic PTR glass fiber optic structures which can be applied in fiber optic devices that require elevated operating temperatures and high optical power levels. Fabrication of a single mode PTR glass fiber with core and cladding is in progress.

References

[1] K. O. Hill and G. Meltz, "Fiber Bragg grating technology fundamentals and overview," *J. Lightw. Technol.*, vol. 15, no. 8, pp. 1263–1276, Aug. 1997.

[2] R. Kashyap, "Fiber Bragg gratings," *J. Lightw. Technol.*, vol. 15, no. 8, pp. 1277–1393, Aug. 1999.

[3] G. Meltz, W. W. Morey, and W. H. Glenn, "Formation of Bragg gratings in optical fibers by a transverse holographic method," *Opt. Lett.*, vol. 14, no. 15, pp. 823–827, 1989.

[4] J. Canning, "Fibre gratings and devices for sensors and lasers," *Laser Photon. Rev.*, vol. 2, no. 4, pp. 275–289, 2008.

[5] D. L. Williams, *et al.*, "Enhanced UV-photosensitivity in boron codoped germanosilicate fibers," *Electron. Lett.*, vol. 29, no. 1, pp. 45–47, 1993.

[6] P. J. Lemaire, *et al.*, "High pressure H_2 loading as a technique for achieving ultrahigh UV photosensitivity and thermal sensitivity in GeO_2-doped optical fibers," *Electron. Lett.*, vol. 29, no. 13, pp. 1191–1193, 1993.

[7] S. R. Baker, *et al.*, "Thermal decay of fibre Bragg gratings written in boron and germanium codoped silica fiber," *J. Lightw. Technol.*, vol. 15, no. 8, pp. 1470–1477, Aug. 1997.

[8] S. Kannan, J. Z. Y. Guo, and P. J. Lemaire, "Thermal stability analysis of UV-induced fiber Bragg gratings," *J. Lightw. Technol.*, vol. 15, no. 8, pp. 1478–1483, Aug. 1997.

[9] I. Riant and B. Poumellec, "Thermal decay of gratings written in hydrogen-loaded germanosilicate fibers," *Electron. Lett.*, vol. 34, no. 16, pp. 1603–1604, 1998.

[10] K. E. Chisholm, K. Sugden, and I. Bennion, "Effects of thermal annealing on Bragg fibre gratings in boron/germanium co-doped fibre," *J. Phys. D*, vol. 31, no. 1, pp. 61–64, 1998.

[11] L. Dong, *et al.*, "Enhanced photosensitivity in tin-codoped germanosilicate optical fibers," *IEEE Photon. Technol. Lett.*, vol. 7, no. 9, pp. 1048–1050, Sep. 1995.

[12] K. Imamura, T. Nakai, Y. Sudo, and Y. Imada, "High reliability tin-codoped germanosilicate fibre Bragg gratings fabricated by direct writing method," *Electron. Lett.*, vol. 34, no. 18, pp. 1772–1773, 1998.

[13] G. Brambilla, V. Pruneri, and L. Reekie, "Photorefractive index gratings in SnO_2:SiO_2 optical fibers," *Appl. Phys. Lett.*, vol. 76, no. 7, pp. 807–809, 2000.

[14] G. Brambilla and H. Rutt, "Fiber Bragg gratings with enhanced thermal stability," *Appl. Phys. Lett.*, vol. 80, no. 18, pp. 3259–3261, 2002.

[15] N. Groothoff and J. Canning, "Enhanced type IIA gratings for high-temperature operation," *Opt. Lett.*, vol. 29, no. 20, pp. 2360–2362, 2004.

[16] J. L. Archambault, L. Reekie, and P. St. J. Russell, "100% reflectivity Bragg reflectors produced in optical fibers by single excimer laser pulses," *Electron. Lett.*, vol. 29, no. 5, pp. 453–455, 1993.

[17] S. J. Mihailov, *et al.*, "Bragg Gratings Written in All-SiO_2 and Ge-doped core fibers with 800-nm femtosecond radiation and a phase mask," *J. Lightw. Technol.*, vol. 22, no. 1, pp. 94–100, Jan. 2004.

[18] A. Martinez, I. Y. Khrushchev, and I. Bennion, "Thermal properties of fibre Bragg gratings inscribed point-by-point by infrared femtosecond laser," *Electron. Lett.*, vol. 41, no. 4, pp. 176–178, 2004.

[19] M. Fokine, "Formation of thermally stable chemical composition gratings in optical fibers," *J. Opt. Soc. Amer. B*, vol. 19, no. 8, pp. 1759–1765, 2002.

[20] S. Bandyopadhyay, *et al.*, "Ultrahigh-temperature regenerated gratings in boron-codoped germanosilicate optical fiber using 193 nm," *Opt. Lett.*, vol. 33, no. 16, pp. 1917–1919, 2008.

[21] L. Glebov. (2007). Fluorinated silicate glass for conventional and holographic optical elements. *Proc. SPIE*, pp. 654507-1–654507-9 [Online]. Available: http://dx.doi.org/10.1117/12.720928

[22] L. B. Glebov, V. I. Smirnov, C. M. Stickley, and I. V. Ciapurin. (2002). New approach to robust optics for hel systems. *Proc. SPIE*, pp. 101–109 [Online]. Available: http://dx.doi.org/10.1117/12.472367

[23] J. Deubener, *et al.*, "Viscosity, relaxation and elastic properties of photo-thermo-refractive glass," *J. Non Crystall. Solids*, vol. 355, no. 2, pp. 126–131, 2009.

[24] G. B. Venus, A. Sevian, V. I. Smirnov, and L. B. Glebov. (2005). High-brightness narrow-line laser diode source with volume Bragg-grating feedback. *Proc. SPIE*, pp. 166–176 [Online]. Available: http://dx.doi.org/10.1117/12.590425

[25] O. Andrusyak, *et al.*, "Spectral combining and coherent coupling of lasers by volume Bragg gratings," *IEEE J. Sel. Topics Quantum Electron.*, vol. 15, no. 2, pp. 344–353, Feb. 2009.

[26] E. Rotari, L. Glebova, and L. Glebov. (2005). Refractive index modulation in photo-thermo-refractive fibers. *Proc. SPIE*, pp. 379–384 [Online]. Available: http://dx.doi.org/10.1117/12.591217